Hindawi Publishing Corporation
Journal of Nanomaterials
Volume 2011, Article ID 869618, 8 pages
doi:10.1155/2011/869618

Research Article

Preparation and Characterization of Pure Rutile TiO_2 Nanoparticles for Photocatalytic Study and Thin Films for Dye-Sensitized Solar Cells

Huei-Siou Chen,[1] Chaochin Su,[1] Ji-Lian Chen,[1] Tsai-Yin Yang,[1] Nai-Mu Hsu,[2] and Wen-Ren Li[2]

[1] *Institute of Organic and Polymeric Materials, National Taipei University of Technology, Taipei 106, Taiwan*
[2] *Department of Chemistry, National Central University, Chung-Li 320, Taiwan*

Correspondence should be addressed to Chaochin Su, f10913@ntut.edu.tw and Wen-Ren Li, ch01@ncu.edu.tw

Received 31 May 2010; Accepted 8 September 2010

Academic Editor: William W. Yu

Pure rutile-phase TiO_2 (r-TiO_2) was synthesized by a simple one pot experiment under hydrothermal condition using titanium (IV) n-butoxide as a Ti-precursor and HCl as a peptizer. The TiO_2 products were characterized by XRD, TEM, ESCA, and BET surface area measurement. The r-TiO_2 were rodlike in shape with average size of $\sim 61 \times 32$ nm at hydrothermal temperature of 220°C for 10 h. Hydrothermal treatment at longer reaction time increased the tendency of crystal growth and also decreased the BET surface area. The degradation of methylene blue was selected as a test reaction to confer the photocatalytic activity of as-obtained r-TiO_2. The results showed a strong correlation between the structure evolution, particle size, and photocatalytic performance of r-TiO_2. Furthermore, the r-TiO_2-based solar cell was prepared for the photovoltaic characteristics study, and the best efficiency of ~3.16% was obtained.

1. Introduction

Titanium dioxide (TiO_2), is one of the most popular and promising materials in the field of photocatalytic applications due to its strong oxidizing power, high photostability, and redox selectivity [1]. When TiO_2 is irradiated by photons with an energy higher than or equal to its band gap (~3.2 eV), through photon absorption, the electrons can be promoted to the conduction band, generating holes in the valence band. The photogenerated electrons and holes migrate to the TiO_2 surfaces where they can induce reduction and/or oxidation of adsorbed molecules. TiO_2 is also a commonly used semiconductor for photon-electron transfer processes. In the dye-sensitized solar cells (DSSCs) invented by Grätzel et al., nanosized TiO_2 particles were used for preparing working electrodes, and the cell performance was found to be improved significantly when compared to the flat layered photoelectrodes [2]. The TiO_2 crystal exists in two major forms: rutile and anatase [3, 4]. Anatase is thermodynamically metastable and can be transformed irreversibly to rutile phase at high temperatures [3, 5]. Most of the chemistry researchers have paid greater attention to anatase TiO_2 than rutile TiO_2 (r-TiO_2) in both photocatalytic reactions and photoelectrochemical cell because anatase phase of TiO_2 had been considered to be more active than rutile. Several excellent properties of r-TiO_2, such as chemical inertness, superior light scattering characteristics, and lower cost [3, 6], however, make it a potentially important phase in photocatalytic and photovoltaic applications. Wang et al. reported the high photocatalytic activity of r-TiO_2 for decomposition of rhodamine-B in water under artificial solar light irradiation [7]. Bacsa and Kiwi found that the presence of r-TiO_2 showed enhanced catalytic activity compared to pure anatase TiO_2 during the degradation of *p*-coumaric acid [8]. Rutile phase has also been shown to be more active than anatase in photodecomposition of H_2S [9], and photooxidation of H_2O with Fe^{3+} [10]. Park et al. showed that the photovoltaic

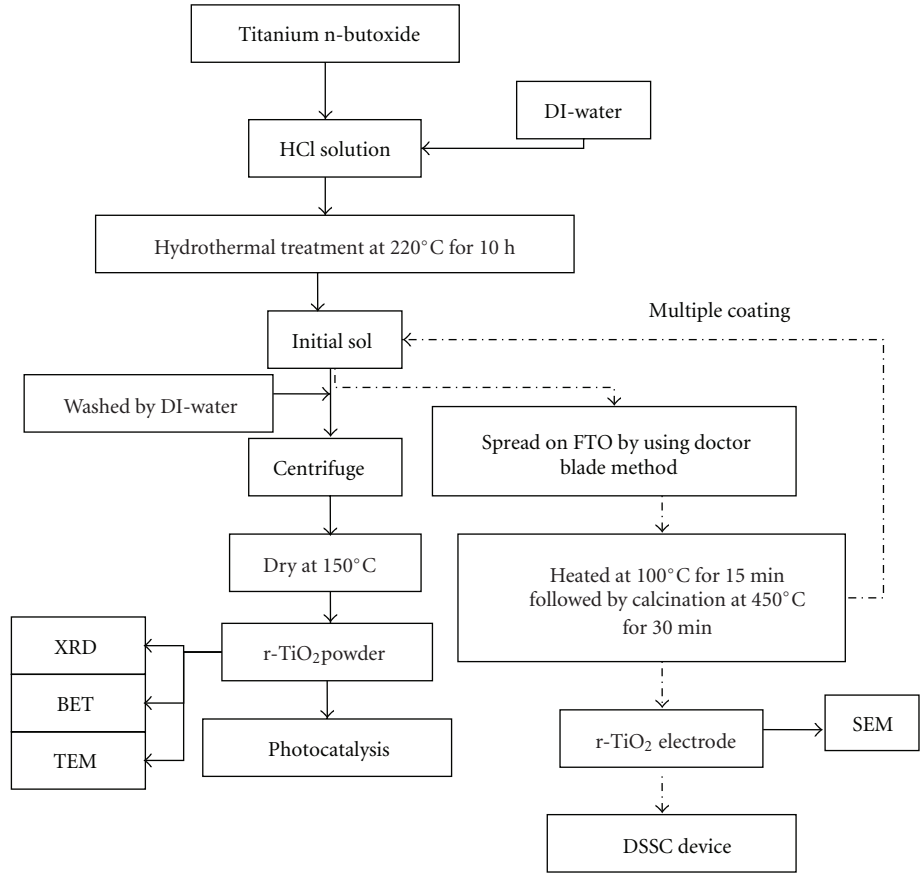

Figure 1: Flow chart of the method for preparing r-TiO_2 by sol-hydrothermal synthesis.

characteristics of rutile TiO_2-based DSSCs are comparable to those of anatase TiO_2-based solar cells [11, 12]. However, due to the insufficient TiO_2 film thickness which is less than 5 μm, the electron injection current and the photon to electron conversion efficiency are limited. It has been proposed that porous film electrodes composed of one-dimensional (1D) nanomaterials provide direct electron conducting channels to the electrodes, thus the solar cell efficiency can be enhanced [13]. Previously, we had successfully prepared the 1D rod-shaped r-TiO_2 nanoparticles by sol-hydrothermal procedure [14]. In continuation of the previous work, we are presenting here with more detailed investigation of the influence of hydrothermal conditions, including the acid concentration and hydrothermal duration on the crystal structure, particle size, particle morphology, and photocatalytic activity of r-TiO_2 nanoparticles. The photocatalytic activity of the derived r-TiO_2 photocatalysts was tested by methylene blue degradation reactions under UV illumination. We also prepared nanocrystalline r-TiO_2 films up to 21 μm in thickness for DSSC study. The effect of r-TiO_2 film thickness and morphology on the photoelectrochemical properties was examined. The overall efficiency of r-TiO_2-based DSSC device is rationalized in terms of r-TiO_2 film thickness and amount of dye adsorbed into the electrodes to find a meaningful property-efficiency correlation.

2. Experimental

2.1. Hydrothermal Synthesis of Rutile TiO_2 Nanorods. Figure 1 shows the schematic diagram for preparing r-TiO_2 nanorods. This procedure is based on the previous sol-hydrothermal process for synthesis of TiO_2 nanoparticles [15] with some modification. Titanium (IV) n-butoxide ($Ti(O\text{-}Bu)_4$, ACROS), as a Ti precursor, was added slowly to hydrogen chloride solution (HCl) under magnetic stirring until a clear sol was formed. Then, distilled water was added dropwise into the sol and continuously stirred for three days. The white mixture formed was then transferred to a Teflon-lined autoclave, 40% filled, and heated at 220°C for various durations. After cooling to room temperature, the products presented in the bottom layer were washed with distilled water several times and finally dried at 150°C to obtain crystallized products. The such-obtained TiO_2 samples were characterized by the transmission electron microscope (TEM, Hitachi, H-7100) for microstructural properties and X-ray diffraction (XRD, Japan MAC Science, MXP 18) for crystalline phase. All peaks measured by XRD analysis were assigned by comparing with those of JCPDS data. The crystal size of the TiO_2 during different states of heat treatment was obtained by the XRD line profile analysis. The Brunauer, Emmett, and Teller (BET) surface area was obtained from nitrogen adsorption-desorption data

(Micromeritics, ASAP-2010). The chemical composition was verified using the electron spectroscopy for chemical analysis (ESCA, VG Scientific ESCALAB 250).

2.2. Photocatalysis by Rutile TiO_2 Nanorods. The photocatalytic reaction was carried out in a custom-made photoreactor (FanChun Technology Inc., PR-2000) [16]. The system is open to air atmosphere with sixteen UV-lamps in total (wavelength 253.7 ± 0.8 nm, Sankyo Denki Co., LTD.) circulating a quartz reaction cell. The power at the position of the reactor center, measured in the air by a power meter (Molectron, PM 150x), was about (1.2 ± 0.2) mWcm^{-2}. UV-Vis spectrometry (JASCO V-630) was used to monitor the absorption spectra of methylene blue (MB) as a function of illumination time. Before the photoreaction experiment, the aqueous solution of MB with initial concentration ($[C_0]$) of 5×10^{-5} mol/l (M) was stirred utterly in the presence of r-TiO_2 sample in the dark to ensure the complete equilibrium of adsorption process. During illumination, a 4 mL aliquot was sampled at various time intervals and centrifuged to separate MB solution for analysis. The photocatalytic efficiencies of the r-TiO_2 samples prepared by hydrothermal treatment for various duration (1, 5, 10, 15, 20, and 24 h) were compared.

2.3. Preparation of Rutile TiO_2 Photoanodes and DSSC Performance Measurement. A doctor-blading technique was used to prepare the r-TiO_2 films on an FTO- (F-doped tin oxide-) coated conductive glass ($2 \times 3.3 \times 0.3$ cm^3, Solaronix, sheet resistance 8 Ωcm^{-2}) as DSSC photoanodes. Two edges of the FTO substrate were covered with Scotch tapes. The r-TiO_2 sol obtained after hydrothermal treatment for 10 h was directly applied to one of the bare edges and flattened with a home-made doctor blade by shearing across the tape-covered edges. The resulted r-TiO_2 electrodes were dried at 100°C for 15 min followed by subsequent calcination at 450°C for 30 min in order to remove the organic residues from the final products and to complete the crystallization. Thickness of the film was controlled by multiple coating process in which the coated substrates were subjected repeatedly to doctor-blade coating, drying, and calcination steps (Figure 1). The thickness of the r-TiO_2 films was measured by a Mahr Alpha-step profiler (Perthometer S2) and confirmed by the scanning electron microscopy (SEM, Hitachi S-2400) images of cross sections. The surface morphology and crystal phase of r-TiO_2 films were investigated by SEM and XRD, respectively.

For photosensitization studies, the r-TiO_2 electrodes with working area of 0.25 cm^2 were immersed in ethyl alcohol containing 3×10^{-4} M N3 dye (Ru[L2(NCS)2], L = 2,2′-bipyridine-4,4′-dicarboxylic acid, Solaronix) for 24 h at room temperature. The Pt counter electrodes with mirror finish were prepared by sputtering deposition (Hitachi E-1045 ion sputter) of a 20 nm layer of Pt on top of FTO substrates. To assemble the DSSC, the electrolyte of 0.5 M LiI (Acros, 99%), 0.05 M I_2 (Showa, 99.8%), 0.5 M 4-*tert*-butylpyridine-TBP (Aldrich, 99%), and 0.5 M 1,2-dimethyl-3-propylimidazolium iodide-DMPII (IonLic-Tech. >98%) in acetonitrile was applied to the Pt electrode, which was then placed over the dye-coated r-TiO_2 electrode to form a sandwich-type clamped cell for photovoltaic study.

The photocurrent versus voltage (I-V) curves were measured using a computerized digital multimeter (Keithley, 2400) under the AM1.5 irradiation (1 sun), provided by a class A Thermo Oriel Xenon lamp light source (300 W). The incident power density was 100 mW cm^{-2} using NREL-calibrated monocrystalline Si-Solar cell (PVM134 reference cell, PV Measurement Inc.) for calibration. The efficiencies were calculated by Forter software.

3. Results and Discussion

3.1. Characterization of Rutile TiO_2 Nanorods. The sol-hydrothermal reaction employed in the present work led to the formation of nanocrystalline TiO_2. The crystal properties depend on the peptization and hydrothermal treatment, such as acid concentration and time period. The previous study showed that using different acids in a hydrothermal reaction resulted in the formation of different TiO_2 phase [17]. The product was pure rutile from an HCl medium, however, if the concentration of HCl was reduced to 1.5 M, besides rutile, anatase phase was generated as a side product. This implied that the formation of anatase by using HCl as a pepitizer was more difficult than that of rutile phase. Based on this result, we selected an HCl concentration of 3 M for the preparation of r-TiO_2 in the study presented here. Figure 2 shows a series of XRD patterns for r-TiO_2 after hydrothermal treatment at 220°C for various duration. For convenience, the r-TiO_2 samples are hereinafter abbreviated as Ht-A-B, where A and B represent the hydrothermal temperature (°C) and heating duration (h), respectively. It can be seen that pure rutile TiO_2 could be successfully obtained with 3 M HCl for the studied hydrothermal period from 1 to 24 hrs. This result infers that the complete formation of rutile phase could be accomplished in the solution at relatively low temperatures under appropriate conditions. In a general sol-gel process for preparing TiO_2, the primary formed structure phase observed at low temperature is anatase which transforms to thermodynamically most stable and more condense rutile phase only upon calcinating at temperature above 500°C [1]. Note that the rutile XRD peaks became sharper as hydrothermal treatment prolonged indicating the formation of larger r-TiO_2. The crystal sizes of r-TiO_2 obtained by analyzing the half maximum (FWHM) of (110) peak at 2θ = 27.45 degree using the Scherrer equation with wavelength of the radiation of 1.5405 Å are summarized in Table 1.

The above XRD results indicate formation of r-TiO_2 crystals that can be confirmed by the ESCA measurement. Figure 3 shows the typical ESCA survey spectra of r-TiO_2 samples. The peaks appearing on the left side showed the Ti2p doublet with bonding energies of 459.4 eV for $Ti2p_{3/2}$ and 464.9 eV for $Ti2p_{1/2}$. The right side spectrum showed the O1s peak with binding energy of 530.4 eV. Those binding energies of Ti2p and O1s from r-TiO_2 samples are all in good agreement with those in standard spectrum of TiO_2. Compared to the individual photoelectron peaks for O1s and Ti2p from nonbonded Ti and O elements, different binding energies due to the chemical shifts were found. The binding

Table 1: The XRD crystal domain, TEM particle size, BET surface area of r-TiO_2 samples, and their photocatalytic activities for photodecomposition of methylene blue in aqueous solution.

r-TiO_2 sample	Domain size (nm)	Particle size in length × width (nm)	BET (m^2/g)	Reaction rate k_a (min^{-1})
Ht-220-1	9.92	26.3×10.8	161.72	7.56×10^{-3}
Ht-220-5	20.58	50.5×18.5	46.73	8.61×10^{-3}
Ht-220-10	25.73	60.9×31.7	35.45	9.29×10^{-3}
Ht-220-15	28.39	71.1×31.0	28.71	1.52×10^{-2}
Ht-220-20	29.41	62.8×31.9	28.44	1.10×10^{-2}
Ht-220-24	31.60	76.9×36.5	18.93	1.04×10^{-2}

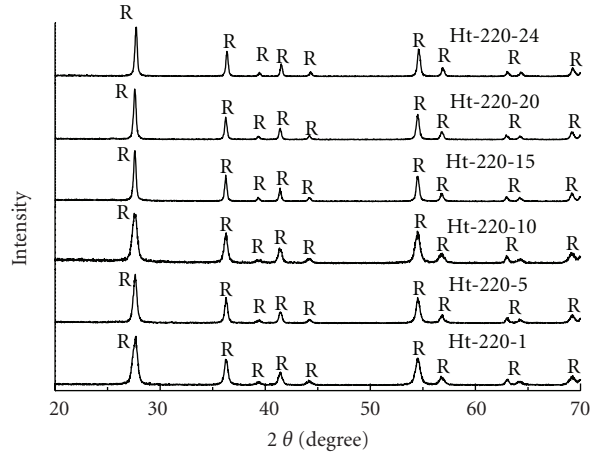

Figure 2: A series of XRD peaks for the prepared r-TiO_2 powders after hydrothermal treatment for various duration.

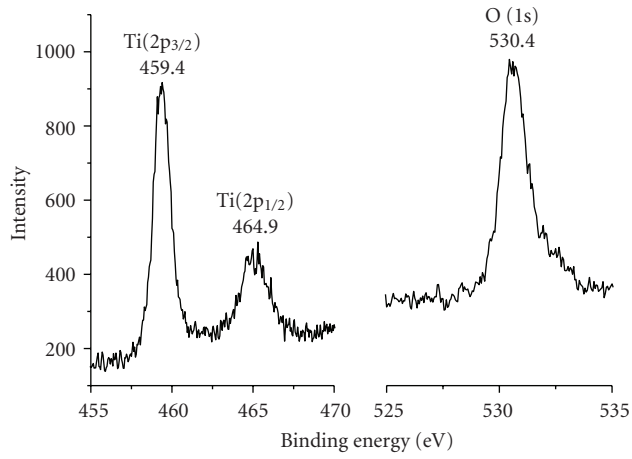

Figure 3: The ESCA spectra of r-TiO_2 sample for Ti 2p (left side) and O 1s (right side).

energy of the core level electron depends critically on the species to which it is bonded. Charge transfer from Ti to O leaves Ti (and O) with partial positive (and negative) charges, leading to a shift in core level to higher ($Ti2p_{3/2}$, 453.7 to 459.4 eV; $Ti2p_{1/2}$, 461.2 to 464.9 eV) and lower (O1s, 531 to 530.4 eV) binding energies associated with increased (and decreased) Coulombic attraction between core electron and the nucleus of Ti (and O) [14].

The crystal growth in different stage of hydrothermal process was traced by TEM. Figure 4 shows the TEM micrographs of r-TiO_2 samples hydrothermally treated at 220°C for (a) 1, (b) 5, (c) 10, (d) 15, (e) 20, and (f) 24 h. As shown in Figure 4, in the initial stage of newly formed TiO_2 sol, the shape of the TiO_2 was observed as elliptical (Figure 4(a)) with average size of 26.3×10.8 nm. Upon increasing the autoclaving time, the r-TiO_2 crystallites build up rod-like morphology progressively. Prolonging the hydrothermal treatment also increases the average particle dimension based on the weighted-average analysis. In other words, increasing autoclaving time promotes the tendency of crystal growth under the present experimental conditions as expected from XRD analysis. In addition, a broad particle size distribution (not shown) was observed in terms of width and length, indicating that the nucleation of r-TiO_2 is much slower than its growth. The range of particle size is from 26.3×10.8 to 76.9×36.5 nm in length × width as listed in Table 1. Nevertheless, the crystals of small size from XRD indicate the incomplete crystallization for hydrothermal treatment up to 24 h.

The size variation of r-TiO_2 can also be seen from BET surface area measurement. The results listed in Table 1 show the dependence of the surface area of r-TiO_2 on the hydrothermal reaction time. It can be seen that the specific surface area shifts towards smaller values for longer heat treatment. The TiO_2 sample with one hour of hydrothermal treatment at 220°C possesses high specific surface area (162 m^2/g) which then decreased appreciably with a limited value around 19 m^2/g after 24 h of hydrothermal treatment. This result confirms the observation from TEM and indicates an increase in the particle size of r-TiO_2 in increasing the reaction time. Obviously, this is due to the progressive aggregation of small crystallites into larger particles. It is known that the TiO_2 crystals grow from TiO_6 octahedra that are terminated by the surface Ti-OH groups. During the hydrothermal treatment under acidic condition, the surface hydroxyl groups can be protonated to form Ti-OH_2^+ which then combines readily with another Ti-OH to form Ti-O-Ti oxygen bridge by eliminating a water molecule (dehydration) through which the crystals grow to a larger size [4]. It is noted that the growth of rutile TiO_2 proceeded via oriented coalescence of the first formed TiO_2 nanorods as demonstrated by many side-by-side aggregated r-TiO_2

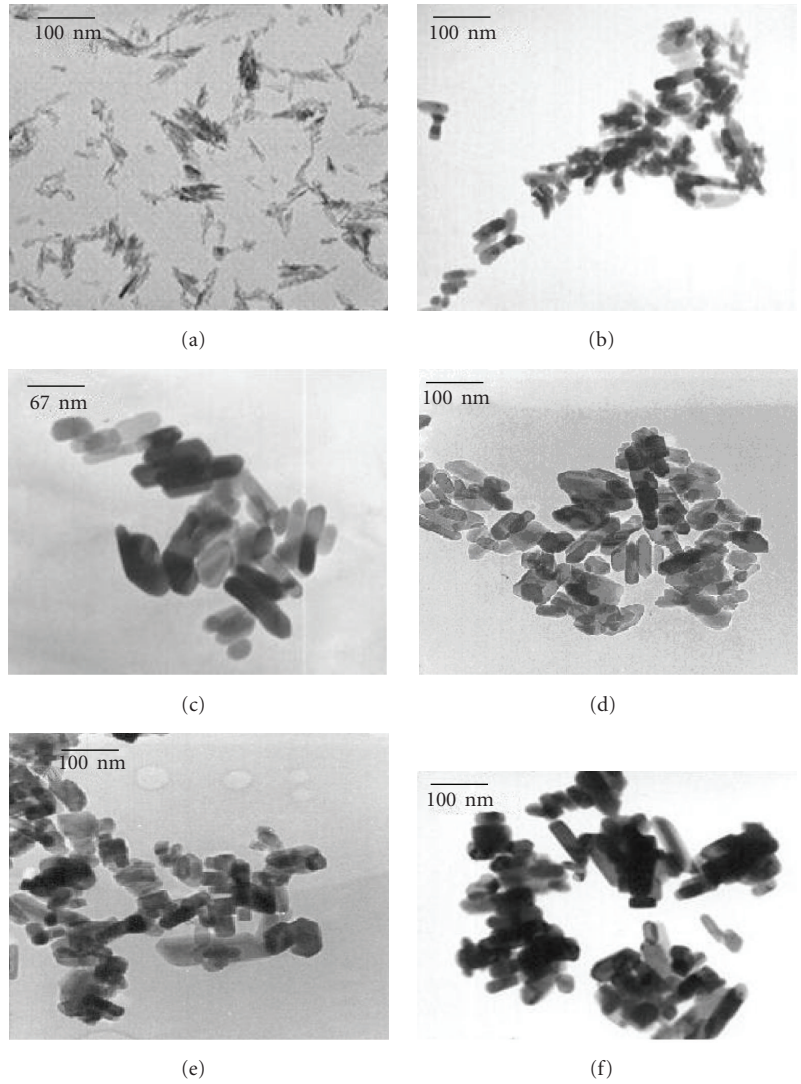

Figure 4: The TEM micrographs of r-TiO_2 samples hydrothermally treated at 220°C for (a) 1, (b) 5, (c) 10, (d) 15, (e) 20, and (f) 24 hrs.

(Figures 4(c)–4(f)) and the simultaneous increase of width and length of r-TiO_2 from TEM analysis.

3.2. Photocatalytic Activity of Rutile TiO_2. In order to study the photocatalytic activity of the above-prepared r-TiO_2, the photodecomposition of methylene blue (MB) was investigated in aqueous heterogeneous suspensions under the acidic condition. We chose pH 3.85 to study the photodegradation of MB because it decomposed scarcely in the absence of TiO_2 upon irradiation up to 7 h [16]. The maximal absorption of MB solutions is at 614 and 664 nm under our experimental conditions. The photodegradation was studied by monitoring the variation of intensity at 664 nm. Figure 5 plots the relative concentration $[C]/[C_0]$ of MB against irradiation time of r-TiO_2 samples prepared by hydrothermal treatment at 220°C for different time period. With r-TiO_2, the MB showed significant decrease in the absorbance upon irradiation. It is noted that varying the hydrothermal-treated period changes the photocatalytic efficiency of r-TiO_2. The photocatalytic activity of r-TiO_2 increases with an increase in hydrothermal time from 1 to 15 h, but it decreases for r-TiO_2 with further hydrothermal treatment (20 and 24 h). There are two major variables that can vary during the hydrothermal process: crystallinity and surface area. Increasing the hydrothermal time increases the crystalline domain of r-TiO_2 based on XRD analysis but decreases the specific surface area based on BET measurement (Table 1). Increase in crystallinity is a positive change in photocatalytic activity since amorphous titania is known to have very low photocatalytic efficiency [1, 18]. Decrease in surface area, on the other hand, is a negative change in photocatalytic activity due to the reduction of surface hydroxyl groups (−OH). The photocatalysis is basically a surface phenomenon that is being very sensitive to the amount of surface OH groups which may act as the principal reactive oxidant in the photoreactions of TiO_2 [19]. To derive the kinetic information, the decay of absorption due to the photodecomposition of MB was tentatively assumed to follow the first-order kinetics:

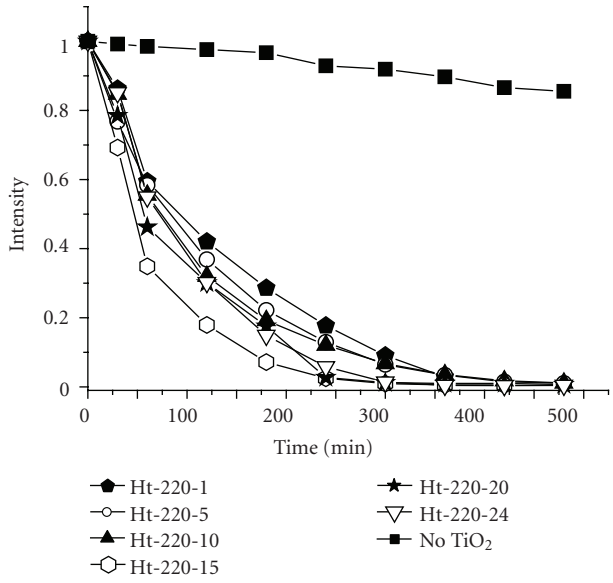

Figure 5: The variation of MB intensity at the $\lambda_{max} = 664$ nm as a function of UV irradiation time in the absence (black solid square) and presence of r-TiO_2 samples prepared for various hydrothermal time.

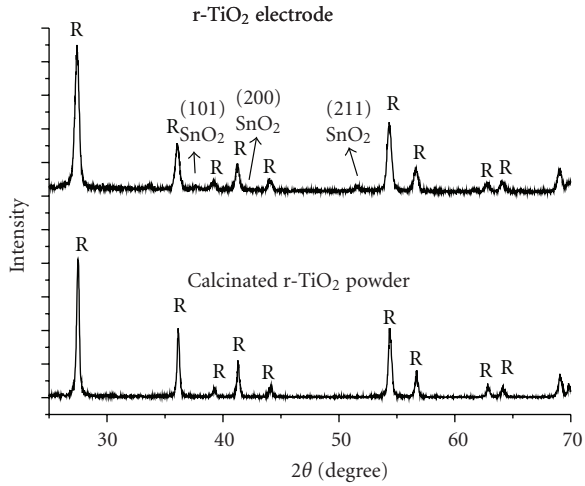

Figure 6: The XRD spectra for r-TiO_2 electrode and r-TiO_2 powder after calcination at 450°C.

rate $= -d[C]/dt = k_a[C]$, where k_a is the apparent rate constant for MB decomposition and $[C]$ is the concentration of MB. To determine the reaction rate constant, curves of the variation of MB concentration as a function of illumination time were fit into this model. The rate constants for photodecomposition of MB using various r-TiO_2 samples are also listed in Table 1. At longer hydrothermal-treated period (up to 15 h), the MB decomposition rate increases which is associated with the improvement of r-TiO_2 crystallinity. Further hydrothermal treatment for more than 20 h, the photocatalysis efficiency of r-TiO_2 is deteriorated, which is believed to be due to the decrease in surface area.

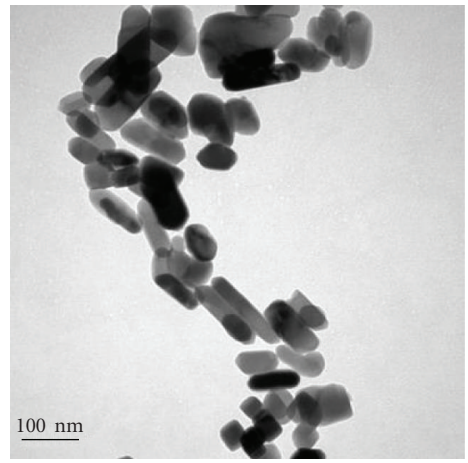

Figure 7: TEM picture of 450°C calcined r-TiO_2 powder.

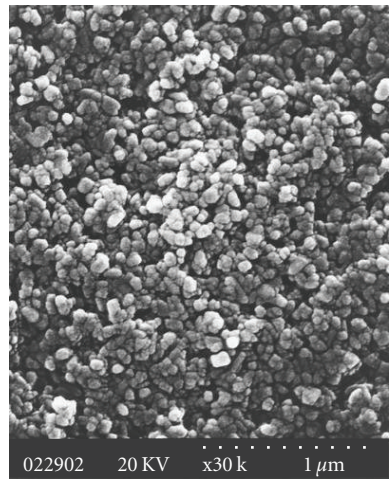

Figure 8: A top-view SEM image of r-TiO_2 electrodes.

3.3. Application of Rutile TiO_2 to DSSCs. DSSC is a quite complicated system, and there are many factors influencing the cell efficiency [20]. One of the most important parameters is the TiO_2 electrode. The crystal phase, particle shape, diameter, and surface composition of TiO_2 samples used will affect the dye adsorption, electron transport, and electrolyte diffusion in the cell as well as the light-to-electricity conversion efficiency. In this work, we chose r-TiO_2 samples obtained after 10 h hydrothermal treatment to prepare the photoanodes for DSSC study because of higher surface area with good crystallinity. As shown in Table 1, the specific surface area shifts towards smaller values for further heat treatment. The film preparation procedure and condition also play significant effect in the resultant electrode property, in particular, the film morphology and porosity. The r-TiO_2 electrodes were prepared according to the procedures described in Section 2.3. The XRD pattern as shown in Figure 6 exhibited peaks corresponding to rutile phase TiO_2 indicating the presence of stable rutile phase after 30 min 450°C calcination. Several small peaks appear at $2\theta = 38.0$, 42.6, and 51.8 are assigned to SnO_2 from

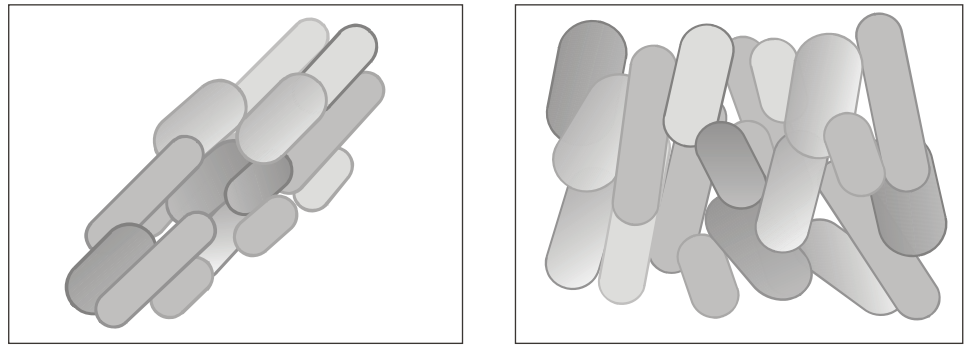

(a) (b)

Figure 9: Model of the crystal enlargement of r-TiO_2 upon calcination on substrate-free (a) and substrate-limited (b) conditions.

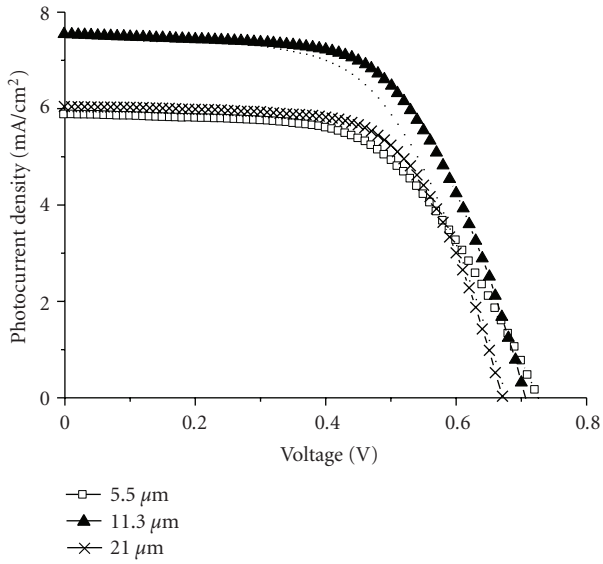

Figure 10: Photocurrent-voltage characteristics of the dye-sensitized solar cells with different thickness of r-TiO_2 films.

Table 2: Performance characteristics of DSSCs based on the r-TiO_2 electrode with different thickness.

Thickness (μm)	J_{sc} (mA/cm^2)	V_{oc} (V)	FF	η (%)	Dye_{ads} (μmole/cm^2)
5.5	5.99	0.73	0.58	2.51	0.22
11.3	7.55	0.70	0.60	3.16	0.28
21.0	6.03	0.67	0.66	2.68	0.40

FTO substrate. In order to see the heat treatment effect on r-TiO_2 morphology, the TEM image was acquired from calcinated r-TiO_2 paste. As shown in Figure 7, the r-TiO_2 powders kept the rod shape morphology even with 450°C calcination process. Contrarily, the rod-like microstructure is somehow diminished on calcinated r-TiO_2 electrodes prepared from the same pastes as shown in Figure 8 from SEM. Only irregular and shorter-rod particles with larger particle size (100 nm) were observed. Although it is not clear why the rod shape can not be kept on r-TiO_2 film, there could be one possible reason as depicted in Figure 9. The surface energy effect is beneficial to the side- (length-) by-side (length) arrangement between rod-shaped r-TiO_2 particles. As mentioned earlier, the growth of rutile TiO_2 proceeded via oriented coalescence of the first formed TiO_2 nanorods. In 3 dimensions, the r-TiO_2 nanorods are freely moved and chances are the simultaneous growth of r-TiO_2 in both length and width directions. On r-TiO_2 film, however, one of the dimensions for r-TiO_2 nanorods to move is limited and only nearby r-TiO_2 nanorods aggregate to form larger but shorter r-TiO_2 particles.

Figure 10 showed the typical current-voltage (J-V) characteristics of N3-sensitized r-TiO_2 solar cells measured at 1 sun light intensity for various r-TiO_2 film thickness. Table 2 lists the photoelectric data, including photocurrent density (J_{sc}), open-circuit voltage (V_{oc}), fill factor (FF), apparent cell efficiency (η), and the dye adsorption density (Dye_{ads}) of the DSSCs in Figure 10. It is generally expected that the DSSC performance largely depends on the TiO_2 film thickness because changing the film thickness changes the amount of dye adsorbed on TiO_2 owing to the change of total TiO_2 surface area. For the homogeneously harvested light by the adsorbed dye molecules, one would also expect the approximately linearly dependence of photocurrent density with the film thickness [21]. It can be seen from Table 2 that when the film thickness increased by 2-fold, from 5.5 to 11.3 μm, the J_{sc} only improved by 26%, from 5.99 to 7.55 mA/cm^2. The increase of J_{sc}, however, is consistent with that of Dye_{ads} which increases ~27%, from 0.22 to 0.28 μmole/cm^2 and that of cell efficiency by ~26% from 2.51 to 3.16. These results indicate that the photocurrent as well as cell efficiency are limited by the number of adsorbed dye molecules for film thickness up to 11.3 μm. A small decrease (5%) of V_{oc} with film thickness may be due to the offsetting effect associated with the J_{sc} and the number of recombination centers on surface area of the film [12]. Further increase of r-TiO_2 film thickness from 11.3 to 21.0 μm, although the amount of dye adsorption increases by 43%, from 0.28 to 0.40 μmole/cm^2, the J_{sc} decreases by 20% from 7.55 to 6.03 mA/cm^2 as well as cell efficiency by ~15% from 3.16 to 2.68. This is due to the increase in the

numbers of recombination centers and the longer mean path of the injected electron to travel inside the cell. Moreover, when the TiO_2 films are thicker, the films become more opaque. Due to the various light absorption mechanism, the irradiation intensity decays significantly upon travelling through the thick films which is therefore detrimental to the DSSC performance [21].

4. Conclusions

Pure rutile phase TiO_2 nanorods have successfully been synthesized under the hydrothermal conditions. Hydrothermal-treated duration shows significant effects on the crystal domain, particle dimension, and photocatalytic activity of r-TiO_2. Hydrothermal treatment at longer reaction time increases the tendency of crystal growth based on TEM/XRD and the BET surface area decreased as well. The photocatalytic activity of r-TiO_2 increases with an increase of hydrothermal time from 1 to 15 h due to the increase of crystal domain, but it decreases for r-TiO_2 with further hydrothermal treatment (20 and 24 h) due to the decrease in surface area. Dye-sensitized solar cells with working area of 0.25 cm^2 were fabricated from various thicknesses of electrode layers made of r-TiO_2 nanorods. The best-performing DSSC evaluated under 1 sun condition gave current density ~7.55 mA/cm^2, open circuit voltage ~0.70 V, fill factor ~60%, and energy conversion efficiency ~3.16%.

Acknowledgments

The authors gratefully acknowledge the financial support from the National Science Council of Taiwan, Republic of China (Contract no. NSC96-2113-M-027-005-MY2). The authors also acknowledge the kind help from Professor H.-W. Fang for film thickness measurement.

References

[1] C. Su, B.-Y. Hong, and C.-M. Tseng, "Sol-gel preparation and photocatalysis of titanium dioxide," *Catalysis Today*, vol. 96, no. 3, pp. 119–126, 2004.

[2] B. O'Regan and M. Grätzel, "A low-cost, high-efficiency solar cell based on dye-sensitized colloidal TiO_2 films," *Nature*, vol. 353, no. 6346, pp. 737–740, 1991.

[3] W. W. So, S. B. Park, K. J. Kim, and S. J. Moon, "Phase transformation behavior at low temperature in hydrothermal treatment of stable and unstable titania sol," *Journal of Colloid and Interface Science*, vol. 191, no. 2, pp. 398–406, 1997.

[4] H. Yin, Y. Wada, T. Kitamura et al., "Hydrothermal synthesis of nanosized anatase and ruffle TiO_2 using amorphous phase TiO_2," *Journal of Materials Chemistry*, vol. 11, no. 6, pp. 1694–1703, 2001.

[5] H. Kominami, J.-I. Kato, S.-Y. Murakami et al., "Synthesis of titanium(IV) oxide of ultra-high photocatalytic activity: high-temperature hydrolysis of titanium alkoxides with water liberated homogeneously from solvent alcohols," *Journal of Molecular Catalysis A: Chemical*, vol. 144, no. 1, pp. 165–171, 1999.

[6] H.-Y. Byun, R. Vittal, D. Y. Kim, and K.-J. Kim, "Beneficial role of cetyltrimethylammonium bromide in the enhancement of photovoltaic properties of dye-sensitized rutile TiO_2 solar cells," *Langmuir*, vol. 20, no. 16, pp. 6853–6857, 2004.

[7] Y. Wang, L. Zhang, K. Deng, X. Chen, and Z. Zou, "Low temperature synthesis and photocatalytic activity of rutile TiO_2 nanorod superstructutes," *Journal of Physical Chemistry C*, vol. 111, no. 6, pp. 2709–2714, 2007.

[8] R. R. Bacsa and J. Kiwi, "Effect of rutile phase on the photocatalytic properties of nanocrystalline titania during the degradation of p-coumaric acid," *Applied Catalysis B: Environmental*, vol. 16, no. 1, pp. 19–29, 1998.

[9] D. D. Beck and R. W. Siegel, "Dissociative adsorption of hydrogen sulfide over nanophase titanium dioxide," *Journal of Materials Research*, vol. 7, no. 10, pp. 2840–2845, 1992.

[10] T. Ohno, D. Haga, K. Fujihara, K. Kaizaki, and M. Matsumura, "Unique effects of iron(III) ions on photocatalytic and photoelectrochemical properties of titanium dioxide," *Journal of Physical Chemistry B*, vol. 101, no. 33, pp. 6415–6419, 1997.

[11] N.-G. Park, G. Schlichthörl, J. van de Lagemaat, H. M. Cheong, A. Mascarenhas, and A. J. Frank, "Dye-sensitized TiO_2 solar cells: structural and photoelectrochemical characterization of nanocrystalline electrodes formed from the hydrolysis of $TiCl_4$," *Journal of Physical Chemistry B*, vol. 103, no. 17, pp. 3308–3314, 1999.

[12] N.-G. Park, J. van de Lagemaat, and A. J. Frank, "Comparison of dye-sensitized rutile- and anatase-based TiO_2 solar cells," *Journal of Physical Chemistry B*, vol. 104, no. 38, pp. 8989–8994, 2000.

[13] Y. Suzuki, S. Ngamsinlapasathian, R. Yoshida, and S. Yoshikawa, "Partially nanowire-structured TiO_2 electrode for dye-sensitized solar cells," *Central European Journal of Chemistry*, vol. 4, no. 3, pp. 476–488, 2006.

[14] C. Su, C.-M. Tseng, L.-F. Chen, B.-H. You, B.-C. Hsu, and S.-S. Chen, "Sol-hydrothermal preparation and photocatalysis of titanium dioxide," *Thin Solid Films*, vol. 498, no. 1-2, pp. 259–265, 2006.

[15] M. Wu, G. Lin, D. Chen et al., "Sol-hydrothermal synthesis and hydrothermally structural evolution of nanocrystal titanium dioxide," *Chemistry of Materials*, vol. 14, no. 5, pp. 1974–1980, 2002.

[16] C. Su, K.-F. Lin, Y.-H. Lin, and B.-H. You, "Preparation and characterization of high-surface-area titanium dioxide by sol-gel process," *Journal of Porous Materials*, vol. 13, no. 3, pp. 251–258, 2006.

[17] Y.-F. Xie, *Preparation and characterization of TiO² by sol-gel from hydrothermal to calcination from nano-powder to nano-film*, M.S. thesis, National Taipei University of Technology, 2006.

[18] B. Ohtani, Y. Ogawa, and S.-I. Nishimoto, "Photocatalytic activity of amorphous-anatase mixture of titanium(IV) oxide particles suspended in aqueous solutions," *Journal of Physical Chemistry B*, vol. 101, no. 19, pp. 3746–3752, 1997.

[19] M. R. Hoffmann, S. T. Martin, W. Choi, and D. W. Bahnemann, "Environmental applications of semiconductor photocatalysis," *Chemical Reviews*, vol. 95, no. 1, pp. 69–96, 1995.

[20] J. Jiu, S. Isoda, F. Wang, and M. Adachi, "Dye-sensitized solar cells based on a single-crystalline TiO_2 nanorod film," *Journal of Physical Chemistry B*, vol. 110, no. 5, pp. 2087–2092, 2006.

[21] K. Hou, B. Tian, F. Li, Z. Bian, D. Zhao, and C. Huang, "Highly crystallized mesoporous TiO_2 films and their applications in dye sensitized solar cells," *Journal of Materials Chemistry*, vol. 15, no. 24, pp. 2414–2420, 2005.